The Response of Yttria Stabilised Zirconia Oxygen Sensors to Carbon Monoxide Gas

V. P. Kotzeva and R. V. Kumar
Department of Materials Science and Metallurgy
University of Cambridge, UK

Abstract. Pressures to reduce pollution and conserve fuel have created a growing interest in emission control, highlighting the need for reliable chemical sensors to detect pollutant gases. With particular regard to automotive emission control, this study examines chemical sensors based on yttria stabilised zirconia (YSZ) solid electrolytes for detection and control of carbon monoxide.

It was found that combustible gases in the exhaust interfere with O_2 measurement when a YSZ oxygen conducting solid electrolyte is used. The detected CO interference on the measurement of O_2 could be utilised in two ways. Firstly, to upgrade the performance of the oxygen sensor in an atmosphere containing combustibles by minimising the effect of the combustibles. Alternatively, the interference can be controlled and quantified for CO detection. Sensors with Pt and Au electrodes were tested in O_2 and CO atmospheres. The measured response was evaluated in relation to theoretical expectations.

1. Introduction

The application of oxygen sensors in the control of air to fuel ratio $\lambda = 1$ is based on the sharp step change of *emf* at the stoichiometric point. This involves the measurement of an open circuit potential, i.e. without flow of electrical current through the cell.

The oxygen sensor can be represented by the electrochemical cell

test gas, Pt | YSZ | Pt, reference air

with the electrochemical reactions

at cathode(+): O_2(reference air) + $4e^- = 2O^{2-}$ (YSZ) (1)

at anode(-): $2O^{2-}$(YSZ) = O_2(test gas) + $4e^-$ (2)

The introduction of CO to the gas mixture changes the response of the sensors drastically, altering the *emf* value, due to a combustion reaction of CO on the surface of the sensor. The interference from combustible gas (CO) on the measurement of O_2 can be used for CO detection, if its response can be quantified [1,2].

Electrochemical oxidation of CO on a Au-Pt electrode on the surface of a zirconia sensor gives a mixed potential [3,4]. The presence of CO or H_2 in air gives mixed potential response not only on YSZ sensor with Ag electrodes [5], but also on gadolinia stabilised ceria sensor with Au-Pt electrodes [6].

In this work, oxygen sensors with Pt and Au electrodes as the working electrode were used to quantify the effects of CO gas.

2. Theoretical Considerations

2.1 Mixed Potential Model. Mixed potentials arise at electrodes, where two reactions occur simultaneously. Based on the concept of the mixed potential theory the electrochemical reaction

$$CO + \tfrac{1}{2}\, O_2 = CO_2 \qquad (3)$$

can be divided into a reduction and an oxidation reaction:

reduction of oxygen $1/2O_2 + 2e^- = O^{2-}$ (4)

oxidation of CO $CO + O^{2-} = CO_2 + 2e^-$ (5)

On the surface of the electrode O_2 molecules react with electrons and produce oxygen anions (Fig. 1). These anions react with the adsorbed CO molecules on the surface of the sensor, releasing electrons. Similar to the common process of corrosion, occurring on metal surfaces, a current is established on the surface of the electrode, at a common mixed potential. Reactions (4) and (5), which are not physically separated, give a mixed electrode potential. They proceed in short circuit at the mixed potential, which has a value intermediate between the equilibrium potential of O_2 and CO. In an open circuit, across the whole cell no net current is allowed to flow, so that at each electrode the sum of the cathodic current must be equal to the sum of the anodic currents [7]. Thus the observed *emf* is the difference between this mixed electrode potential and the equilibrium electrode potential of the reference electrode.

At the electrode surface, when the rate of oxidation and the rate of reduction become equal, a dynamic equilibrium is achieved. A measure of this dynamic equilibrium is the reaction constant. It can be measured as the exchange current density (i_o). The expression is a rearrangement of Faraday's Law:

$$K_{ox} = K_{red} = i_o/zF \quad (6)$$

where K_{ox} and K_{red} are reaction constants for the oxidation and reduction reactions, i_o is the exchange current density, and z and F are the number of electrons in the reaction and the Faraday constant respectively.

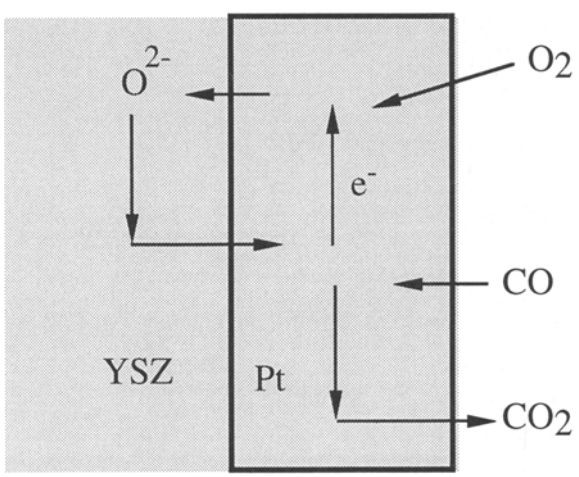

Fig. 1. Mixed potential.

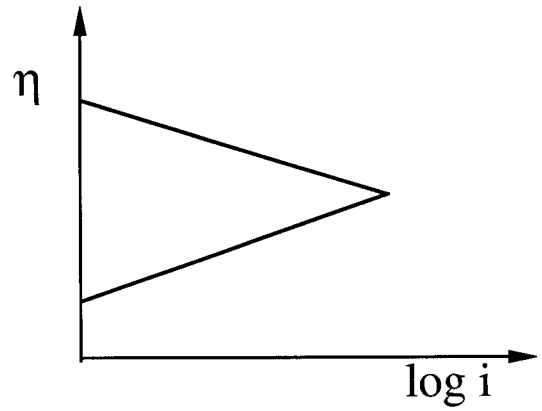

Fig. 2. Tafel lines.

In order to sustain the oxidation/reduction reaction, the energy barrier that exists in the electrical double layer at the electrode/electrolyte interface must be overcome. An overpotential (η) is required, which is a kinetic value resulting from an electrode reaction rate. The relationship between this overpotential and the reaction rate is given by the Tafel equation,

$$\eta = a + b \log i \quad (7)$$

where $b = 2.303RT/\sigma zF$ and $a = -2.303RT/\sigma zF \log i_o$. α is a symmetry factor.

If the equation is presented graphically in a half logarithmic scale, the relationship between the potential and the current density is shown as a linear function (Fig. 2).

2.2. Diffusion Limited Process. Fig. 3 illustrates the three phase boundary of the sensor, when the process is diffusion limited. The example treats O_2, but similar arguments can apply to CO or any other gas. When the distribution of oxygen molecules in the gas phase near the electrode surface is relatively uniform, the Tafel eq. (7) and Fig. 2 describe the process. If the region becomes deficient of oxygen molecules, a limiting rate will be

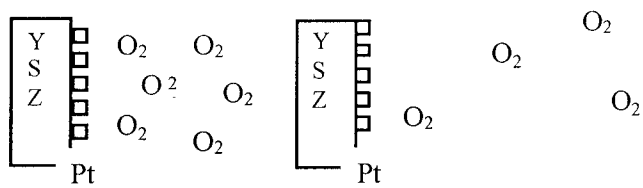

Fig. 3. Concentration gradients during diffusion limited process.

reached, which is determined by the diffusion rate of the oxygen molecules to the electrode surface. This limiting rate is the limiting diffusion current density (i_L). It is a function of the diffusion coefficient (D) of the reacting molecules, their concentration (C_{bulk}) in the bulk of the gas and of the thickness of the diffusion layer (x):

$$i_L = DzF\ C_{bulk}/x \tag{8}$$

Changes in the involved parameters will influence the limiting diffusion current density. The shape of the electrode and the available agitation determines the thickness of the diffusion layer. Figure 4 shows the graphical representation of eq. (9) for the overpotential (η), when the process is diffusion limited:

$$\eta = 2.303(RT/zF)\ \log\ (1\text{-}i/i_L) \tag{9}$$

2. Experimental Description

To evaluate the response of sensors with different electrodes two sensors were tested. They were made from 3 mol% Y_2O_3 stabilised zirconia, in a thimble shape with gold or platinum coating outside and a platinum electrode inside. The inside electrode was exposed to air as a reference gas. The test gas mixture was supplied from a gas blender with a constant flow rate of 400 $cm^3 \cdot min^{-1}$. The gases fed into the blender were high purity oxygen and 30% CO in N_2. High purity Ar was also used as diluent. The experiments were carried out at three fixed concentrations of O_2. The concentration of CO was varied.

3. Results and Discussion

3.1. Response to Oxygen. According to the Nernst equation

$$emf = (2.303RT/4F)\log pO_2^{ref}/pO_2^{test} \tag{10}$$

where R is the Gas constant ($8.314\ Jmol^{-1}K^{-1}$) and F is the Faraday constant ($96500As\ mol^{-1}$).

The reference electrode, exposed to air only, works as an oxygen electrode and its potential is fixed under a constant O_2 concentration ($pO_2 = 0.21$ atm). At the sensing electrode O_2 and other constituents of the gas mixture can undergo electrode reactions at the three-phase contact between the electrolyte, porous electrode and test gas. Each sensor was heated up to the operating temperature. Both sensors were maintained at 897 K working temperature. Most commercially available Lambda sensors do not report zero *emf* at $pO_2 = 0.21$ atm, resulting in offsets which arise due to temperature gradients [8]. Using calibration the equation describing each of the sensors was obtained. For the sensor with two Pt electrodes the relationship is

$$emf = -47.9 - 44.5 \lg pO_2 \tag{11}$$

For the sensor with one Au and one Pt electrode

$$emf = -39.9 - 44.5 \lg pO_2 \tag{12}$$

3.2. Response to CO. The response of the sensors to a pO_2/pCO ratio at the partial pressures of oxygen used in the experiment is shown in Figs. 5, 6 and 7. In order to understand the difference in response of Pt or Au electrode sensors the results are presented using the molar ratio of O_2 to CO for the reaction (3).

The input gas stoichiometric requirement for complete combustion is given by

$$pO_2 / pCO = 1/2. \tag{13}$$

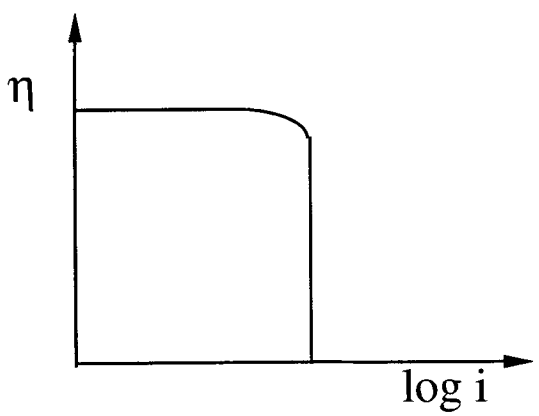

Fig. 4. Diffusion limited process.

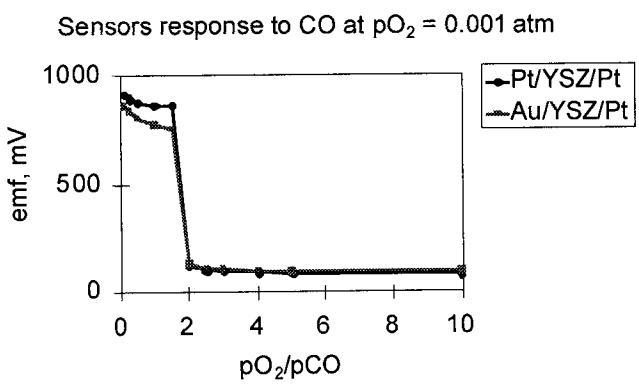

Fig. 5. Sensor's response to CO at $pO_2 = 0.001$ atm.

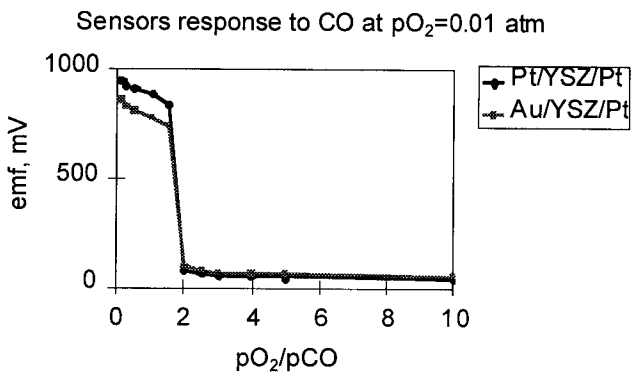

Fig. 6. Sensors response to CO at pO_2= 0.01 atm.

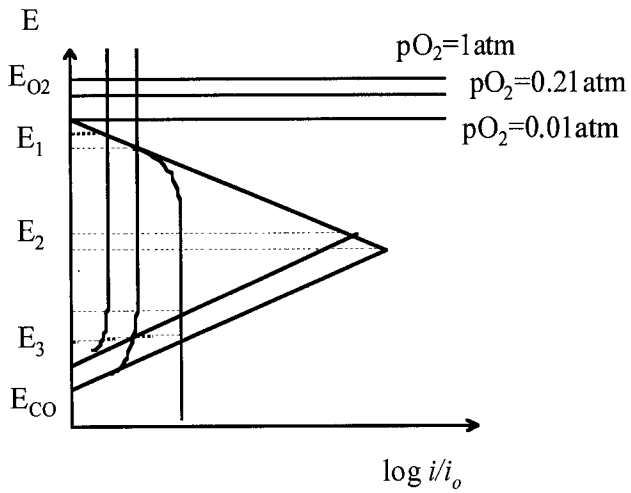

Fig. 7. Mixed potential model predictions.

According to the above requirement, the *emf* would be low at $pO_2/pCO > 1/2$ and high at $pO_2/pCO < 1/2$. At low partial pressure of O_2 (pO_2 = 0.001 atm) the sharp change of the *emf* value for all tested sensors occurs at $pO_2/pCO = 2$. At pO_2 = 0.01 atm the sharp response for both sensors occurs at $pO_2/pCO = 2$.

Assuming that complete combustion takes place on the surface of the sensor, two moles of CO react with one mole of O_2 at the stoichiometric point. From the experimental data obtained for a given pO_2, it was deduced that $pCO = 1/2\ pO_2$, which means that a reaction of only 0.5 moles of CO is sufficient to bring the partial pressure of O_2 on the sensor's surface to the equilibrium ($pO_2 < 10^{-20}$ atm).

From the mixed potential considerations there are three theoretically possible *emf* responses (Fig.7):

If $pO_2 >> pCO$, then the *emf* value would be given by the intersection of the CO/CO_2 diffusion limited line and the oxygen concentration limited line (E_1). The increase of temperature tends to shift the lines towards a decrease of the *emf* value in the E_1 region. The low *emf* value from the experiment with $pO_2 >> pCO$ is in good agreement with the predictions for E_1.

If $pO_2 = pCO$, then the *emf* value would be given by the intersection of the CO/CO_2 Tafel line and the oxygen Tafel line (E_2), or by the intersection of the CO/CO_2 Tafel line and the oxygen diffusion limited line (E_3). No *emf* values in E_2 region were observed in the experiment. The high measured values of *emf* indicate an oxygen diffusion limited process.

Another oxygen diffusion limited reaction occurs when $pCO > pO_2$. Under these conditions the expected *emf* value would be E_3. In both cases the measured *emf* value would be high, which agrees with the experimental data.

3.3. Calculation of the Mixed Potential Model. From the experimental data and the mixed potential model discussed above, calculations were performed in order to quantify the model.

For sensors, where both compartments are insulated, the air oxygen content at the reference electrode fixes the equilibrium electrode potential. In the model this equilibrium potential is presented as a straight line parallel to the abscise.

At pO_2 = 1atm from the equations for each of the sensors (11) and (12) the offset of each of the sensors is calculated. The highest cathodic value is obtained when pO_2 is 1 atm. For simplicity we set this value as 0. To present the potential as a reduction potential Em, the *emf* with reversed sign value is taken:

$$Em = - emf \qquad (14)$$

To present all other potentials in correlation with this starting point and to correct for the offset for the sensor, from each reduction potential Em the value of the measured potential at 1 atm (Em_1) needs to be subtracted. The new value presents the theoretical potential Et for a given partial pressure of oxygen.

$$Et = Em - Em_1 \qquad (15)$$

When the concentration of CO in the test gas is high, the oxygen potential will be determined by the equilibrium

reaction constant for reaction (3) at the working temperature of the sensor:

$$K = \frac{pCO2}{pCO \times \sqrt{pO2}} \tag{16}$$

Assuming that the partial pressures of carbon monoxide and carbon dioxide are equal, then the equilibrium reaction constant (K = $2.34 \cdot 10^{12}$ at 897 K) relates directly to the partial pressure of oxygen in the system. This could be used for calculation of the concentration of oxygen

$$K = \frac{1}{\sqrt{pO2}} \tag{17}$$

For the reduction reaction of oxygen the electrode potential E can be calculated from the difference between the equilibrium potential Eo and the overpotential for the given partial pressure of oxygen:

$$E = Eo - \frac{2.303RT}{4F} \log \frac{1}{pO2} \tag{18}$$

Replacing the values for the sensors Eo = 0 and pO_2 calculated from (17) gives maximum theoretical value for Et max = -1101 mV.

The oxygen concentration is fixed at 0.1, 0.5 or 1 %. However, the CO concentration for these three oxygen concentrations is variable, ranging from 0 to 1, 0 to 5 and 0 to 10% respectively. At high pCO the expression $pCO \times \sqrt{pO2}$ = constant is used for determination of the partial pressure of oxygen for a given partial pressure of carbon monoxide:

$$\log pCO + \frac{1}{2} \log pO2 = const. \tag{19}$$

The difference between any two values of pO_2 can be calculated from eq. (19)

$$\Delta \log pO2 = -2\Delta pCO \tag{20}$$

The shift of the Tafel lines for different partial pressures of oxygen will be parallel and the value for the next potential can be calculated from the relationship

$$\Delta E = 44.5 \Delta \log pO2 \tag{21}$$

We have shown how to calculate all potentials as reduction potentials for the given concentration of oxygen for a mixed potential model.

The starting point of the Tafel lines can be the ordinate value equal to i_o, assuming i_o is the same for both electrodes. This assumption is reasonable, taking into account that both electrodes are made of platinum.

Further simplifying the model is the assumption that the symmetry factor α is equal to 1/2. This allows easy calculation of the Tafel line for the reduction process on the cathode

$$\eta_c = -\frac{2.303RT}{\alpha zF} \log \frac{i}{io} \tag{22}$$

or calculated for the sensors

$$\eta = 178 \log \frac{i}{i_O}. \tag{23}$$

The Tafel line for the oxidation process on the anode is

$$\eta_a = +\frac{2.303RT}{\alpha zF} \log \frac{i}{io} \tag{24}$$

or calculated for the sensors

$$\eta = -178 \log \frac{i}{io}. \tag{25}$$

At the cross point

$$Ec = Ea \tag{26}$$

both Tafel lines have the same slope of 178 mV/ $\log(A \cdot m^{-2})$. The intersection will be

$$E = \frac{Eco - Eo_2}{2} \tag{27}$$

The oxidation Tafel line for the highest concentration of CO starts at Et max, calculated from (18) on the basis of the equilibrium constant of the reaction (Fig. 7). The second point is the cross point at E, calculated from (27) for each of the experimental concentrations of oxygen. With these two points the oxidation Tafel line is determined. For each of the other concentrations of CO, the

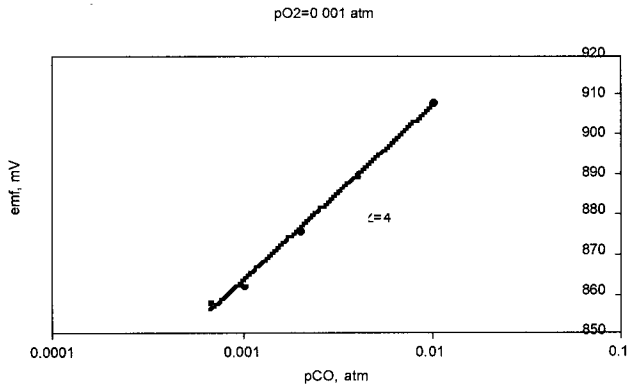

Fig. 8. High *emf* versus pCO for Pt/YSZ/Pt sensor at pO_2 = 0.001 atm.

first point on the y-axis is determined by Et max + ΔE from (21). The lines are parallel to each other. The experimental value for the maximum Et is different. It will lie on the cross point of the oxidation Tafel line and oxygen diffusion limited reduction line. By plotting the value on the oxidation Tafel line, the place of the reduction line is fixed. For each CO concentration the points will lie on the same line. The model predictions for the *emf* are given by the difference between the cross point of oxidation and reduction lines and the potential of the reference (air) electrode.

When the concentration of CO is relatively low in the test mixture, the process becomes CO diffusion limited. The theoretical *emf* is determined as the difference between the theoretical potential and the potential of the reference electrode. For all the low experimental concentrations of CO the points will lie on the oxygen reduction Tafel line on a distance from the reference air line equal to the theoretical *emf*. These points are the cross point of the oxygen reduction Tafel line and the CO diffusion limited oxidation line. If the process was not CO diffusion limited, the theoretical potential, calculated on the basis of the pO2 and the reaction constant (18) will give the value on the y-axis. The line will be parallel to the other lines.

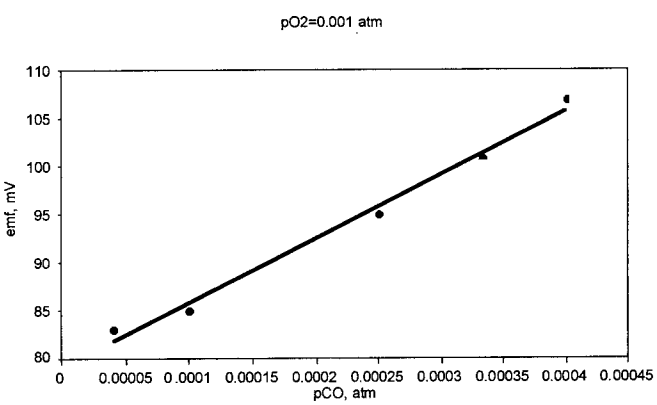

Fig. 9. Low *emf* versus pCO for Pt/YSZ/Pt sensor at pO_2 = 0.001 atm.

When the experimental high *emf* values, corresponding to the oxygen diffusion limited current, meet the CO oxidation Tafel line (Fig. 7), then the corresponding i_L limits can be identified on the diagram. For different concentrations of CO the oxidation Tafel line shifts according to eq. (20) and (21), which is Nernstian behaviour. At one of the experimental concentrations, when pO_2 is fixed at 0.001 atm, the *emf* values versus pCO for high and low *emf* are presented in Figs. 8 and 9. 0.01 atm the nominal Nernst slope gives a calculated $z = 4$.

When the experimental low *emf* values, corresponding to the CO diffusion limited current, meet the O_2 reduction Tafel line (Fig.7), then the corresponding i_L limits can be identified. In the same example as above, for CO concentrations in range $4x10^{-5}$ to $4x10^{-4}$ atm, the correlation between the *emf* and pCO is linear.

4. Summary

The effect of CO gas on the responses of two oxygen sensors at three fixed concentrations of O_2 was investigated. The experimental results are explained in terms of the mixed potential model.

The response of YSZ oxygen sensors to carbon monoxide in the presence of oxygen, showed that catalytically active Pt electrodes give a higher *emf* than less catalytically active Au electrodes, due to CO/O_2 reaction.

The knowledge and understanding of the CO interference on the measurement of O_2 could be utilised in two ways. Firstly, to minimise its effects by change of the temperature and the electrode, thus improving the performance of the oxygen sensor in atmospheres, containing combustibles. Alternatively, the oxygen sensor could be used for CO detection, by quantifying and controlling the effect.

5. References

[1] H. Okamoto, H. Obayashi and T. Kudo, Solid State Ionics **1**, 319 (1980).

[2] E. Häfele, K. Kaltenmaier and U. Schönauer, Sensors and Actuators B **4**, 525 (1991).

[3] Z. Lukasc, M. Sinz, G. Staikov, W.J. Lorenz, G. Baier and A. Vogel, Solid State Ionics **68**, 93 (1994).

[4] T. Hibino, Y. Kuwahara and S. Wang, Journal of The Electrochemical Society **146**, 382 (1999).

[5] H. Kaneko, H. Taimatsu, Y. Miyoshi, K. Kawanaka and T. Kusano, Sensors and Actuators B **13-14**, 151 (1993).

[6] R. Mukundan, E. Brosha, D. Brown and F. Garzon, Electrochemical and Solid State Letters **2**, 412 (1999).

[7] P. Moesley, J. Norris and D..Williams, (eds) Techniques and Mechanisms in Gas Sensing, Adam Hilger, Bristol 1 (1991)

[8] R.W. Gibson, R.V. Kumar and D.J. Fray, Solid State Ionics **121,** 43 (1999).

Paper presented at the 6th Euroconference on Solid State Ionics, Cetraro, Calabria, Italy, Sept. 12-19, 1999.

Manuscript rec. Sept. 16, 1999; acc. Oct. 20, 1999.